Earth and Planetary Science Letters 289 (2010) 30–42

Contents lists available at ScienceDirect

Earth and Planetary Science Letters

journal homepage: www.elsevier.com/locate/epsl

Investigation of the age and migration of reversing dunes in Antarctica using GPR and OSL, with implications for GPR on Mars

C.S. Bristow [a,c,*], P.C. Augustinus [b], I.C. Wallis [b], H.M. Jol [b,c], E.J. Rhodes [d]

[a] School of Earth Sciences, Birkbeck College, University of London, Malet Street, London WC1E 7HX, UK
[b] School of Geography, Geology and Environmental Science, The University of Auckland, Private Bag 92019, Auckland, New Zealand
[c] Department of Geography and Anthropology, University of Wisconsin-Eau Claire, 105 Garfield Avenue, Eau Claire, WI 54702-4004, USA
[d] Department of Environmental and Geographical Sciences, Manchester Metropolitan University, Chester Street, Manchester, M1 5GD, UK

ARTICLE INFO

Article history:
Received 19 June 2009
Received in revised form 7 October 2009
Accepted 17 October 2009
Available online 26 November 2009

Editor: T. Spohn

Keywords:
seasonal
climate
reworking
topographic steering
Mars analogue

ABSTRACT

GPR provides high resolution images of aeolian strata in frozen sand in the McMurdo Dry Valleys of Antarctica. The results have positive implications for potential GPR surveys of aeolian strata on Mars. Within the Lower Victoria Valley, seasonal changes in climate and a topographically-constrained wind regime result in significant wind reversals. As a consequence, dunes show reversing crest-lines and flattened dune crests. Ground-penetrating radar (GPR) surveys of the dunes reveal sets of cross-strata and low-angle bounding surfaces produced by reversing winds. Summer sand transport appears to be dominant and this is attributed to the seasonal increase in solar radiation. Solar radiation which heats the valley floor melts ice cements making sand available for transport. At the same time, solar heating of the valley floor generates easterly winds that transport the sand, contributing to the resultant westward dune migration. The location of the dune field along the northern edge of the Lower Victoria Valley provides some shelter from the powerful föehn and katabatic winds that sweep down the valley. Topographic steering of the winds along the valley and drag against the valley wall has probably aided the formation, migration and preservation of the dune field. Optically-stimulated luminescence (OSL) ages from dune deposits range from 0 to 1.3 kyr showing that the dune field has been present for at least 1000 yr. The OSL ages are used to calculate end-point migration rates of 0.05 to 1.3 m/yr, which are lower than migration rates reported from recent surveys of the Packard dunes and lower than similar-sized dunes in low-latitude deserts. The relatively low rates of migration are attributed to a combination of dune crest reversal under a bimodal wind regime and ice cement that reduces dune deflation and restricts sand entrainment.

1. Introduction

Antarctica is the coldest, driest and windiest continent on Earth. In the areas free of snow and ice, liquid water only flows in streams for around two months each year during the austral summer. However, winds blow throughout the year so that aeolian sediment transport is probably more important than fluvial transport. This is most evident in the Victoria Valley, one of the McMurdo Dry Valleys of Antarctica (Fig. 1), where there is a variety of types of sand dunes including transverse, barchanoid, and whaleback dunes, in addition to proto-dunes, embryonic dunes, sand-sheets and sand-ramps (Lindsay, 1973; Calkin and Rutford, 1974; Selby et al., 1974; Miotke, 1985; Bourke et al., 2009; Bristow et al., 2009). In this paper we focus on the Packard dunefield, which is located along the northern margin of the Lower Victoria Valley beneath the Packard Glacier (Fig. 1). The Lower Victoria Valley is around 15 km long and trends east to west. At its eastern end lies the Victoria Lower Glacier and at its western end is Lake Vida. The valley slopes from east to west from the toe of the Victoria Lower Glacier at around 400 m to Lake Vida at 350 m elevation above sea level (ASL). The valley walls are steep and rise to elevations of between 1000 and 1500 m ASL.

The first published report of the Victoria Valley dunefield was part of a wider investigation of the regional geology by Webb and McKelvey (1959), who described the dunes as barchan and longitudinal types formed under the influence of east–west winds. Research interest in the Victoria Valley dunes was stimulated in the early 1970's when the dunes were investigated by Morris et al. (1972a,b) as part of a geomorphological study that aimed to collect data for visual comparison with images expected from the Viking Mars Mission which was launched in1975, arriving at Mars in 1976. Further geomorphic and sedimentary studies of the dunes were undertaken by Lindsay (1973); Calkin and Rutford (1974); Selby et al. (1974); Miotke (1985); Speirs et al. (2008) and Bourke et al. (2009).

The dunes in the Victoria Valley are potential analogues for dunes on Mars because the low temperatures and high aridity are analogous to the surface conditions on Mars where a variety of dune forms have

* Corresponding author.
E-mail address: c.bristow@ucl.ac.uk (C.S. Bristow).

0012-821X/$ – see front matter © 2009 Elsevier B.V. All rights reserved.
doi:10.1016/j.epsl.2009.10.026

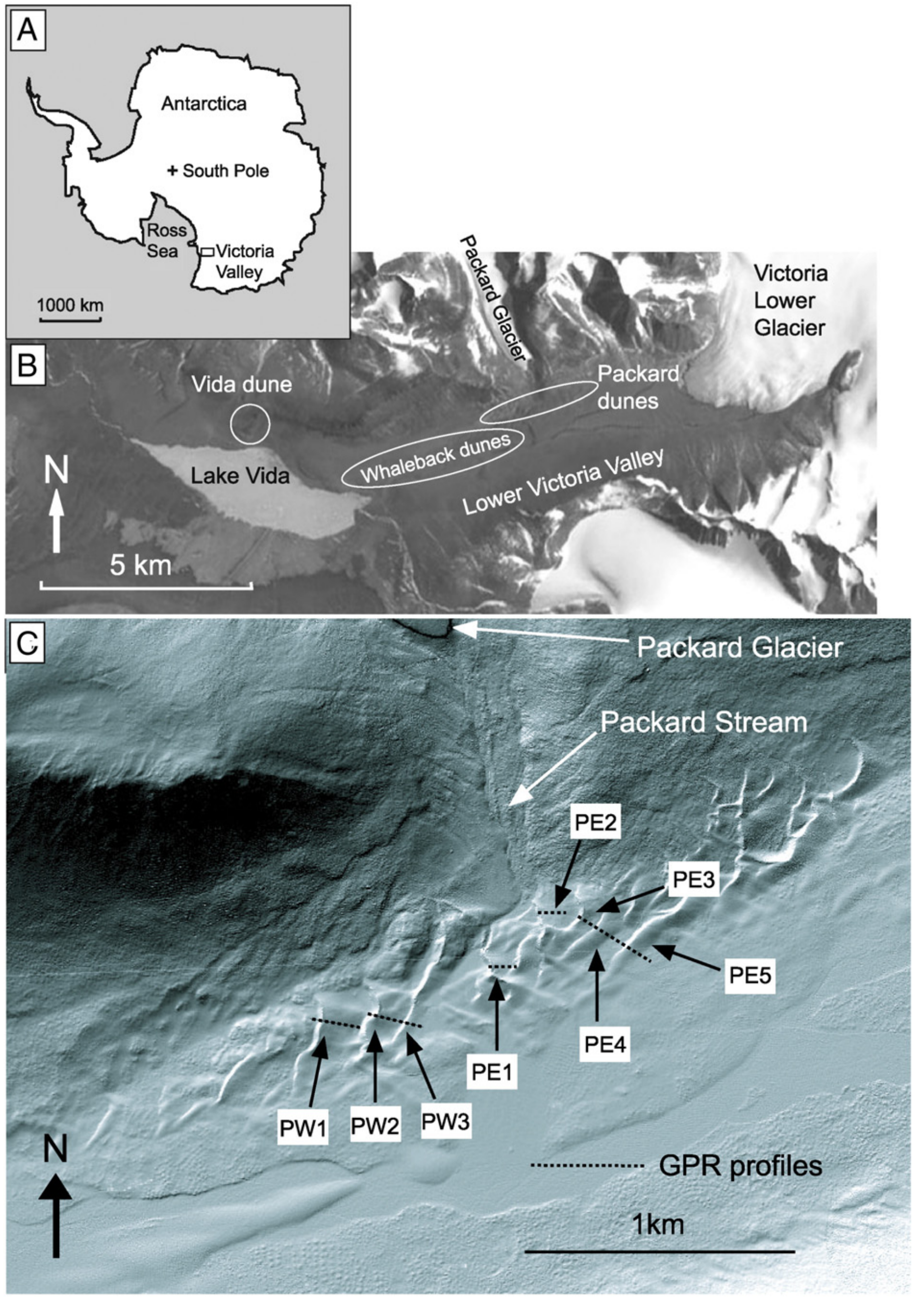

Fig. 1. A) Map of Antarctica showing location of the McMurdo Dry Valleys. B) Satellite image of the Lower Victoria Valley showing the dunefields. C) LiDAR image of the Packard dune field in the Lower Victoria Valley showing the location of the GPR profiles across the dunes that are described in this paper. The dunes described are labelled PW1–3 for those west of the Packard stream and PE1–5 to the east of the Packard stream.

been observed (Malin et al., 1998; Hayward et al., 2007) including reversing transverse dunes and barchanoid dunes with reversing crest-lines (Fenton et al., 2005). The success of the Mars Exploration Rovers, Spirit and Opportunity, and high resolution images of the Martian surface have created renewed interest in the geology and surface processes operating on Mars (e.g.; Squyres et al., 2004a,b; Grotzinger et al., 2005). The European Space Agency (ESA) ExoMars mission planned for launch in 2013 will include a rover which will carry ground-penetrating radar (GPR) as part of the Pasteur payload. The WISDOM (Water Ice and Subsurface Deposit Observation on Mars) instrument will be the first space borne GPR on a rover (Plettemeier et al., 2009). The WISDOM experiment plans to characterise the soils on Mars and then map their variability such as alluvial or aeolian layering (Ciarletti et al., 2009). GPR has previously been deployed within the McMurdo Dry Valleys for Mars analogue studies (Arcone et al., 2002), and in this paper we present a detailed analysis of aeolian strata of sand dunes in the Lower Victoria Valley imaged by GPR.

The Victoria Valley dunes are also potential analogues for the extensive mid-latitude periglacial aeolian deposits of the Northern Hemisphere (e.g. Koster, 1988; Seppälä, 2004). Although cold climate dunes are now recognised in many parts of the northern hemisphere (Good and Bryant, 1985; McKenna-Neuman and Gilbert, 1986; Koster, 1988; Koster and Dijkmans, 1988; Dijkmans, 1990; Mann et al., 2002; Mountney and Russell, 2004; Bateman and Murton, 2006) their structures remain poorly documented. This may be due in part to the presence of permafrost which prevents excavation of trenches. However, ice is no barrier to GPR and the structure of cold climate dunes can be successfully imaged using this approach, as we demonstrate in this paper.

The aims of this paper are to describe and interpret the structure of cold climate dunes as revealed by (GPR) profiles across the Packard dunefield in the Victoria Valley, Antarctica. These profiles should provide a template for comparison with potential GPR images of aeolian strata on Mars. In addition, we investigate the effects of seasonal wind reversals on the dunes in Victoria Valley that have been noted previously (Lindsay, 1973; Selby et al., 1974). We present images of the internal structure of reversing dunes for which there is almost no data from either warm or cold deserts. This is despite the fact that reversing dunes are one of the nine types of dune defined by McKee (1979). In addition, we will use optically-stimulated luminescence (OSL) to constrain the age of the sand dunes and calculate rates of dune migration. We compare these rates with earlier estimates from aerial photograph interpretation and field monitoring and discuss the local climatic controls on dune migration.

2. The Packard dune field

The Packard dunefield is located on the northern side of the Lower Victoria Valley beneath the Packard Glacier (Fig. 1). According to Bourke et al. (2009) the dune field is about 3.1 km long and covers an area of 1.5 km^2. It includes over 30 dunes, most of which are barchanoid or transverse (Fig. 1) although some are climbing dunes ascending till ridges on the valley margin (Fig. 2). Topographic profiles across the dunes show that the dune height varies between 3.3 and 12.1 m while the width varies from 46 to 136 m at the time of our survey in November 2006 (Table 1). These figures compare with results from LiDAR interpretation whereby Bourke et al. (2009) determined an average dune height of 5.3 m with a range from 1.8 to 11 m. Their approach to measuring dune length and height differ from ours because they measured the stoss-side width, and dune height was estimated from the LiDAR data set by selecting the highest point on the dune crest or brink and a point at the foot of the avalanche slope and calculating the difference (Bourke et al., 2009). Note that the apparent elevations on the LiDAR dataset are incorrect but the relative elevations are believed to be reasonably accurate.

A meltwater stream from the Packard Glacier flows into the Packard dune field and for convenience we informally use the stream to divide the dunes into two parts, west of the Packard stream and east of the Packard stream. The crests of the dunes are oriented northeast to southwest oblique to the valley. To the west of the Packard stream the dune crest-line is closer to north–northeast to south–southwest probably influenced by the orientation of underlying till ridges (Fig. 2).

Table 1
Dune height and width at the time of the surveys in November and December 2006.

Dune	Height (m)	Width (m)
PE1	9.8	100
PE2	5.5	76
PE3	7.3	92
PE4	7.8	68
PE5	7.8	92
PW1	12.1	136
PW2	9.1	100
PW3	3.3	46

The dunes reverse due to seasonal changes in the wind strength and direction (Lindsay, 1973; Selby et al., 1974). In the summer months the winds are dominantly from the east and the dunes develop west facing slip-faces. During the winter months strong westerly winds reshape the dunes blowing sand and snow from west to east. The westerly winds are described as katabatic winds draining from the Polar Plateau (Nylen et al., 2004) but an alternative suggestion is that they are aerodynamically deflected upper level winds that produce a föehn effect (e.g. McKendry and Lewthwaite, 1992; McGowan and Speirs, 2008; Speirs et al., 2009). The westerly winds are most frequent in the winter and less common in the summer, whilst in the winter the westerly winds are stronger than those in the summer (Nylen et al., 2004). Both the summer easterly winds from the Ross Sea and the westerly katabatic or föehn winds are topographically-channelled along the valley (Doran et al., 2002; Ayling and McGowan, 2006).

East dipping sets of interbedded sand and snow strata dipping towards the east, in the direction opposite to that of the dune slip-face are reported by Lindsay (1973), Selby et al. (1974) and Miotke (1985). They suggest that these sets of cross-stratification formed by westerly winds during the winter. The contrast between field observations of

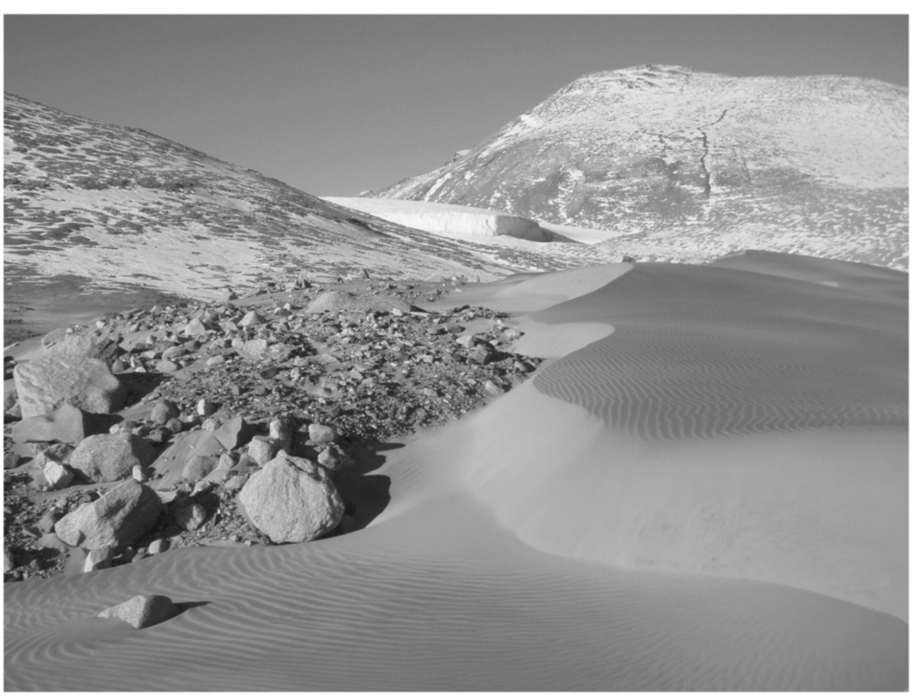

Fig. 2. Transverse climbing dune with a northwest facing slip-face (PW3), migrating onto a till ridge, with the Packard Glacier in the background (December 5th 2006).

west facing slip-faces during the summer months and trenches that reveal east dipping strata (e.g. Miotke, 1985, Fig 18 pg. 101) suggests that the dunes may have a complex internal stratigraphy with many reactivation surfaces due to seasonal wind reversals. In addition, monitoring of a small barchan dune by Speirs et al. (2008) shows that reversals can occur in a matter of days. Speirs et al. (2008) recorded changes in the crest-line of a dune that migrated east at a rate of 2.25 m/day under a westerly wind and then reversed back at a rate of 1.67 m/day under an easterly wind over a period of five days.

3. Field observations

At the time of the surveys in November–December 2006 the top of the dunes were free of snow and covered by a layer of fine sand and wind ripples. Beneath the surface the sand was locally cemented by ice but most of the dune was dry frozen and sometimes interbedded with snow layers. The dry frozen sands were sufficiently well consolidated for wind deflation to produce small outcrops of frozen sand at the dune crest (Miotke, 1985). These sands would remain frozen at night but usually soften during the day when solar radiation increased and thawed interstitial ice. Once thawed, the sand was more easily mobilised and eroded revealing fresh layers of frozen sand. Thus, the potential for aeolian sediment transport tended to increase through the day with increasing surface temperatures driven by solar radiation. Warming of the valley floor also helps to generate easterly “sea breezes” that blow inland from McMurdo Sound (McKendry and Lewthwaite, 1992). Solar radiation is driving both potential sediment mobility, by melting frozen sand, and increasing aeolian sediment transport by generating easterly winds during the summer months.

4. Ground-penetrating radar

Ground-penetrating radar (GPR) has been used successfully to image the internal structures of a variety of desert and coastal sand dunes (e.g. Bristow et al., 1996, 2000a,b, 2005, 2007). GPR works well in dune sands because they have a low conductivity and contain large-scale sedimentary structures that can be imaged by GPR (Bristow, 2009). In this study GPR profiles were collected along and across eight of the dunes in the Packard dune field using a PulseEKKO 1000 with 900 and 450 MHz antennas and a PulseEKKO 100 with 100 and 200 MHz antennas, all in bistatic mode. The GPR profiles in this paper were all collected using a PulseEKKO 100 with 200 MHz antennas, a step size of 0.1 m, antenna separation 0.5 m, in parallel broadside configuration, with the exception of PE1 which was collected with 100 MHz antennas, spaced at 1 m, with 0.25 m step size.

Topographic elevations were measured at 5 m intervals along the profiles and at breaks in slope using a Geodimeter 620 Total Station survey instrument. Topographic corrections have been applied to the GPR data. For depth estimates we have used a velocity of 0.15 m/ns calculated from CMP surveys on the dunes which indicate velocities between 0.14 and 0.17 m/ns. These velocities are consistent with published velocities for dry sand 0.12–0.17 m/ns and ice 0.17 m/ns (Reynolds, 1997). Around 3.2 km of data was collected across five dunes to the east of the Packard Stream (PE1–5) and three to the west of the stream (PW1–3). Data processing included Ekko trace fix, Dewow, AGC gain maximum 100, and migration.

5. Optically-stimulated luminescence

Twelve samples of dune sand were collected for OSL dating in opaque tubes pushed horizontally into the wall of small hand dug pits at depths of between 0.3 and 0.9 m. Sample locations were selected based upon the interpretation of bounding surfaces identified on the GPR profiles. The OSL ages are used below to calculate the end-point migration rates for the dunes based upon the sample's age and the horizontal distance to the slip-face on the lee-side of the dune following the method of Bristow et al. (2005). A further sample of surface sand was collected from the active parts of a dune. The samples were processed under dark room conditions with sand-sized quartz grains separated using dry sieving and magnetic separation techniques, followed by etching for 60 min in concentrated HF to remove the outer alpha-irradiated surface of each grain. Each sample was subsequently resieved to remove grain fragments.

Initial luminescence measurements were conducted to assess signal characteristics and sensitivities. These determinations revealed that the samples displayed OSL and TL (Thermoluminescence) characteristics typical of quartz, though with an extremely low OSL sensitivity. No IRSL (Infra Red Stimulated Luminescence) signal above background was observed for any of the samples, indicating successful removal of feldspar grains.

A single aliquot regenerative-dose (SAR) protocol was used for dating (Murray and Wintle, 2000, 2003; Wintle and Murray, 2006). For insensitive quartz samples from glacial environments, potential problems can be caused by thermal transfer during the preheating steps of the dating protocol (Rhodes and Pownall, 1994; Rhodes, 2000). This effect can give rise to significant apparent age over-estimates when higher preheat temperatures are used. In order to avoid these problems, preheat plateau experiments were conducted for two samples, using both natural and optically-zeroed OSL signals (Rhodes, 2000). A preheat treatment of 10 s at 180 °C prior to natural and regenerative OSL measurements, and a heating step of 10 s at 160 °C before each OSL sensitivity measurement were selected on the basis of these experiments. The full dating protocol, incorporating these preheat treatments was tested using recovered dose experiments (Wintle and Murray, 2006), providing results in agreement with the administered doses, and increasing our confidence in the validity of these age estimates.

As mentioned above, these samples displayed very low OSL signal sensitivity. This prevented us using single grain measurements to assess the degree of signal zeroing during grain transport prior to burial during dune formation. Measurements were made using 12 aliquots each comprising grains adhered to the central 5 mm of 10 mm diameter stainless steel discs using silicone oil, except for samples PD 4 and MD 1C where low quartz yields limited us to 9 and 3 aliquots respectively. Some samples displayed significant variation (beyond the uncertainties caused by counting statistics) between the dose estimates of each aliquot, in the form of several higher dose values. This observation demonstrates that this measurement procedure can detect incomplete zeroing, and we expect that larger multigrain aliquots increase the chance of including rare sensitive grains. Dose values from outlying aliquots were rejected from the analysis (Rhodes, 2007), and the signals from the remaining consistent aliquots were summed to produce a single composite regenerative growth curve and natural value for each sample. The resulting dose estimate and associated uncertainty values were used in the age calculations.

Environmental dose rates were estimated using ICP-MS determinations of sediment U and Th concentration, and ICP-AES for K, using the conversion factors of Adamiec and Aitken (1998). Beta attenuation was estimated using the values of Mejdahl (1979) and ice content attenuation used the equations of Aitken (1985) for water, assuming that the *in situ* values were representative of the burial period. Cosmic dose rate contributions were calculated from sediment overburden thickness using the equations of Prescott and Hutton (1994).

The uncertainties for each age estimate represent 1 sigma (68%) uncertainty limits. For some samples these are large owing to the very low counts observed for the natural OSL, caused by very low signal sensitivities and young burial ages. All age estimates are quoted in years before AD 2007 (Table 2).

Table 2
Optically-stimulated luminescence sample ages.

Sample	Lab code	Depth (m)	Age (thousands of years before AD 2007)	1 sigma error (thousands of years)
PD2	K1855	0.8	1.30	±0.13
PD3	K1856	0.46	0.16	±0.02
PD4	K1857	0.59	0.15	±0.06
WP1C	K1858	0.33	0.27	±0.12
WP1D	K1859	0.33	0.28	±0.05
WP1E	K1860	0.53	0.05	±0.01
WP1Fb	K1861	0.73	−0.09	±0.10
WP2	K1862	0.52	0.07	±0.09
WP3	K1863	0.80	0.09	±0.03

6. Results

6.1. Eastern Packard dune PE1

PE1 is the tallest of the dunes that we surveyed in the eastern half of the Packard dune field, standing 9.8 m above the interdune surface. It has a flat top and is relatively symmetrical although the west facing slope is slightly steeper than the east facing slope (Fig. 3). Based upon the geomorphology alone it is difficult to determine which is the stoss and lee-side of the dune, or which way it has migrated. The 100 MHz GPR profile shows inclined reflections dipping towards the west (Fig. 4). These reflections are interpreted as bounding surfaces between sets of cross-stratification, with the westward dip indicating that the dune has been migrating from east to west so that the dominant dune-forming wind is from the east. It is apparent that the west facing slope of the dune has been reshaped by westerly winds to form the bounding surfaces. The bounding surfaces are preserved by sand deposited during the summer easterly winds when the west facing side of the dune becomes the lee-side visible in Fig. 3. An inclined reflection dipping towards the east near the crest of the dune is interpreted as a set of cross-strata dipping towards the east (Fig. 4). This indicates deposition on the east facing dune slope formed during westerly winds.

The sand is most likely to have been reworked from the west face as it is reshaped and deposited on the east side of the dune which is the lee-side with respect to westerly winds. The symmetry of the dune and the inclined reflections on the GPR profile provides evidence for the dune migration and deposition under the bimodal wind regime. The dominant dune-forming wind is from the east, which has resulted in westward migration of the dune as indicated by the west dipping cross-strata, but westerly winds reprofile the west facing dune surface and lead to reversal of the crest (Fig. 4). There has been limited reworking of the east facing slope and crest-line because the dune is partly frozen and the ice-cemented sand resists wind deflation. Ice-cemented strata are visible on the top of the dune in Fig. 3.

6.2. East Packard dunes PE3 and PE4

Dunes PE3 and 4 are a compound dune form comprising two transverse dunes both oriented NE–SW and with NW facing slip-faces, but with one transverse dune (PE4) migrating onto the other transverse dune (PE3) (Fig. 5). In the trough between the two dunes there was an area of nivation deformation structures including snow hummocks, sinkholes, tension cracks and snow meltwater fans. These structures are similar to those observed by Koster and Dijkmans (1988) at the Great Kobuk Sand Dunes in Alaska where seasonal melting of snow layers produces niveo-aeolian deformation structures. Snow layers interbedded with aeolian sands have been described in the Packard dune field by Lindsay (1973), Calkin and Rutford (1974), Selby et al. (1974), and Miotke (1985). We encountered snow layers up to 40 cm thick in most of the trenches excavated for OSL sample collection. In this location a layer of snow appears to have accumulated in the lee of the dune slip-face because most of the deformation structures were located along the base of the slip-face at the interface between the two dunes. Seasonal melting of snow layers at the time of the survey appeared to be localised at the base of NW facing slip-faces. Melting snow has locally disturbed the reflection patterns of some of the GPR profiles which are interpreted as denivation structures (e.g. Figs. 5 and 6).

The 200 MHz GPR profile across dune PE3 shows inclined reflections and a basal sub-horizontal reflection (Fig. 5). The inclined reflections dip towards the NW with differing inclinations. The steeper dipping reflections are interpreted as sets of cross-stratification. The lower-angle inclined reflections that truncate underlying inclined reflections and are downlapped by overlying inclined reflections are interpreted as bounding surfaces. These bounding surfaces are interpreted as redefinition/reactivation surfaces, as described by Kocurek (1996), formed by reshaping of the dune during reversing westerly winds and downlapped as the NW facing slip-face reformed in response to easterly summer winds. Southeast

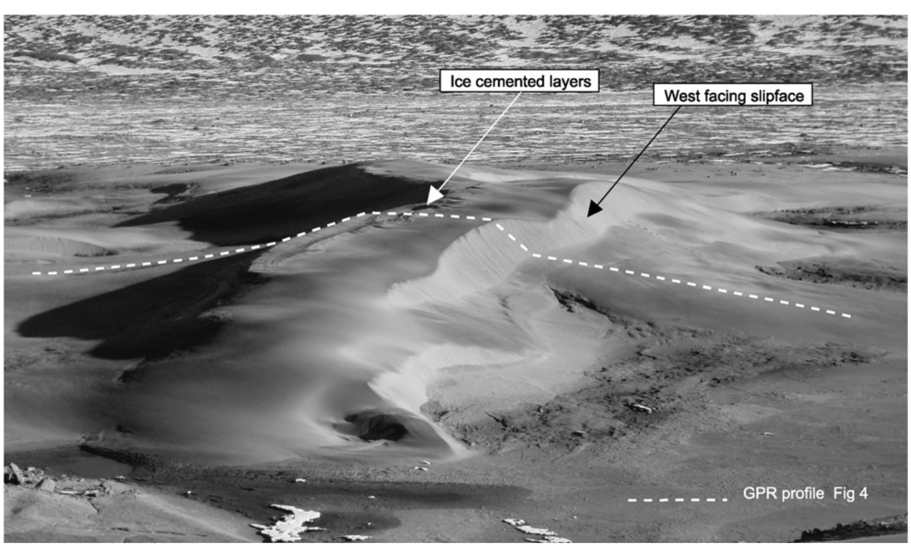

Fig. 3. View facing south across the Packard stream towards dune PE1, a reversing dune with a flat top, and displaying slip-face development on both sides. The west facing ‘summer’ slip-face is visible on the right side of the dune. The slip-face is prograding over a surface that was reshaped by westerly winds. The GPR profile across this dune is shown in Fig. 4 (December 5th 2006).

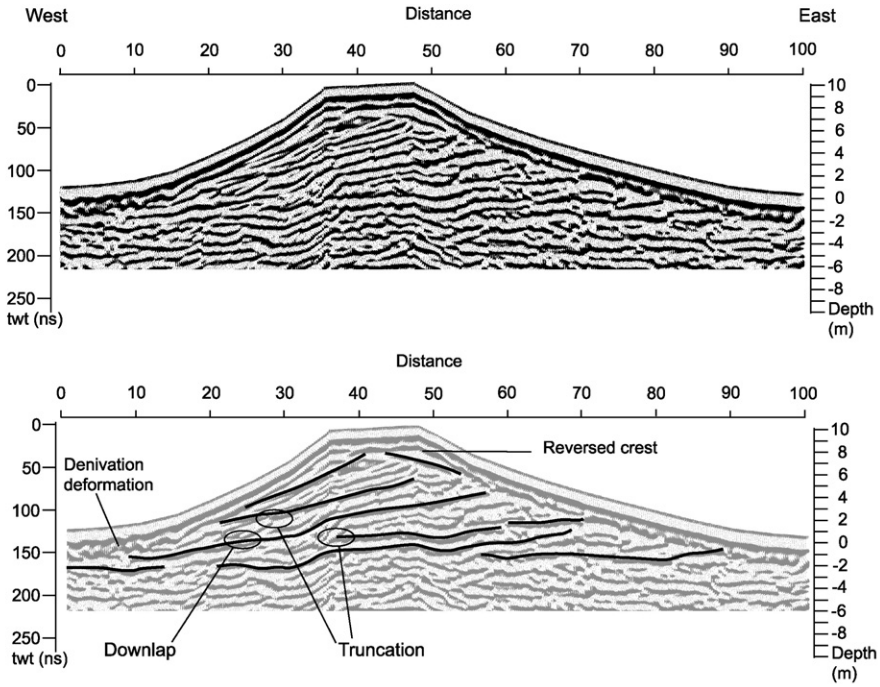

Fig. 4. GPR profile (100 MHz) across dune PE1 showing the symmetrical profile and flat top that is a consequence of reversing winds. Inclined reflections within the dune dip towards the west, showing that this is the direction of dune migration. The surfaces highlighted in the interpretation diagram are bounding surfaces formed when the dune was reshaped. Inclined reflections from cross-strata downlap onto the bounding surfaces and are truncated by them. One inclined reflection close to the dune crest is dipping towards the east and is interpreted to result from the dune crest reversing under westerly winds. Most reflections dip towards the west, indicating dune migration from east to west, driven by east winds. Vertical exaggeration ×1.6.

dipping reflections on the stoss-side of the dune are interpreted as sand layers reworked from the dune crest and deposited during the previous winter. An OSL sample from a depth of 0.8 m at 92 m along the GPR profile gives an age of 1.3 ± 0.13 kyr (Fig. 5). This is the oldest age for any of our samples from the Packard dunes. Projecting this age to the dune slip-face at 22 m along the GPR profile indicates that the dune has migrated ca. 70 m within the past 1300 yr giving an end-point migration rate of ca. 0.05 m/yr.

The GPR profile across dune PE4 shows inclined tangential reflections dipping towards the NW (Fig. 5). The inclined reflections are interpreted as sets of cross-stratification that downlap onto a bounding surface formed by erosion in the lee of the dune as it

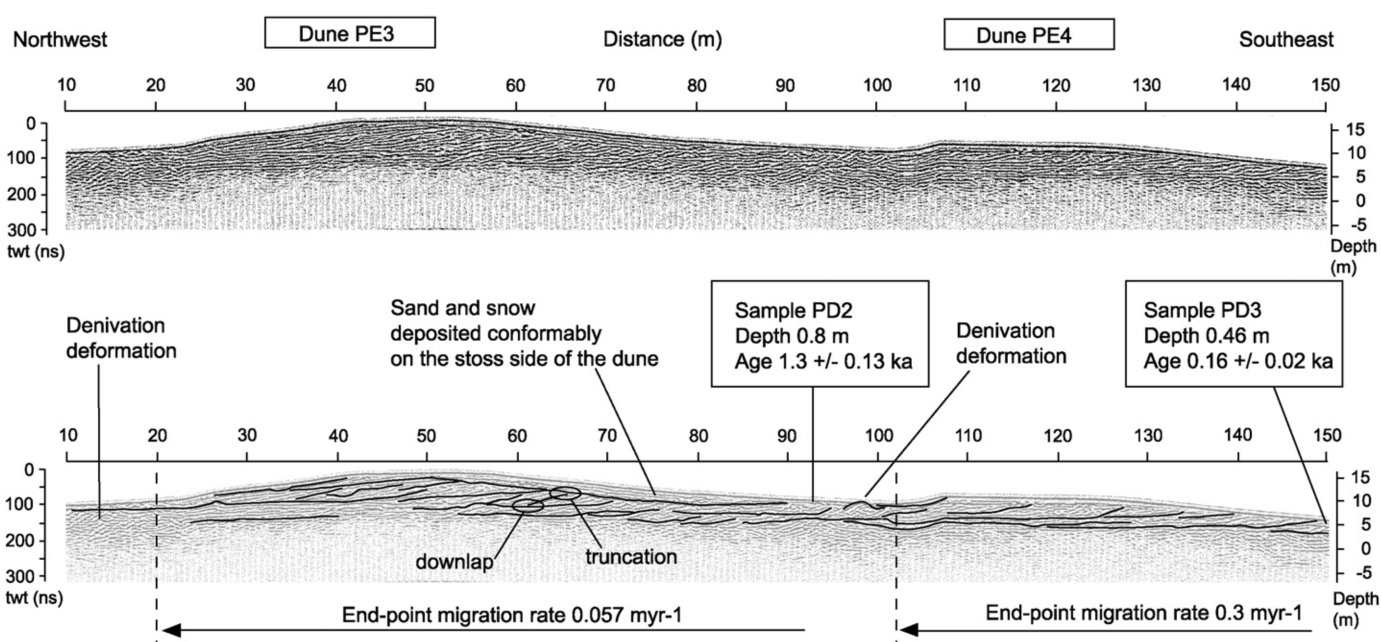

Fig. 5. PE3 and PE4 are transverse dunes, with PE4 superposed on the stoss-side of PE3. Both dunes are migrating from SE to NW, as evidenced by inclined reflections dipping towards the NW on the GPR profile. Low-angle inclined reflections are bounding surfaces formed when the dune was reshaped by reversing winds. Reflections from cross-strata that downlap onto the bounding surfaces represent the former lee-side of the dune. Conformable reflections on the stoss-side of dune PE3 are interpreted as beds of snow and sand deposited on the stoss-side of the dune by westerly winds. Rates of dune migration have been calculated for each dune based upon the age of OSL samples collected from the trailing edge of each dune and the distance to the slip-face where sediment is accumulating at the present day. Vertical exaggeration ×2.

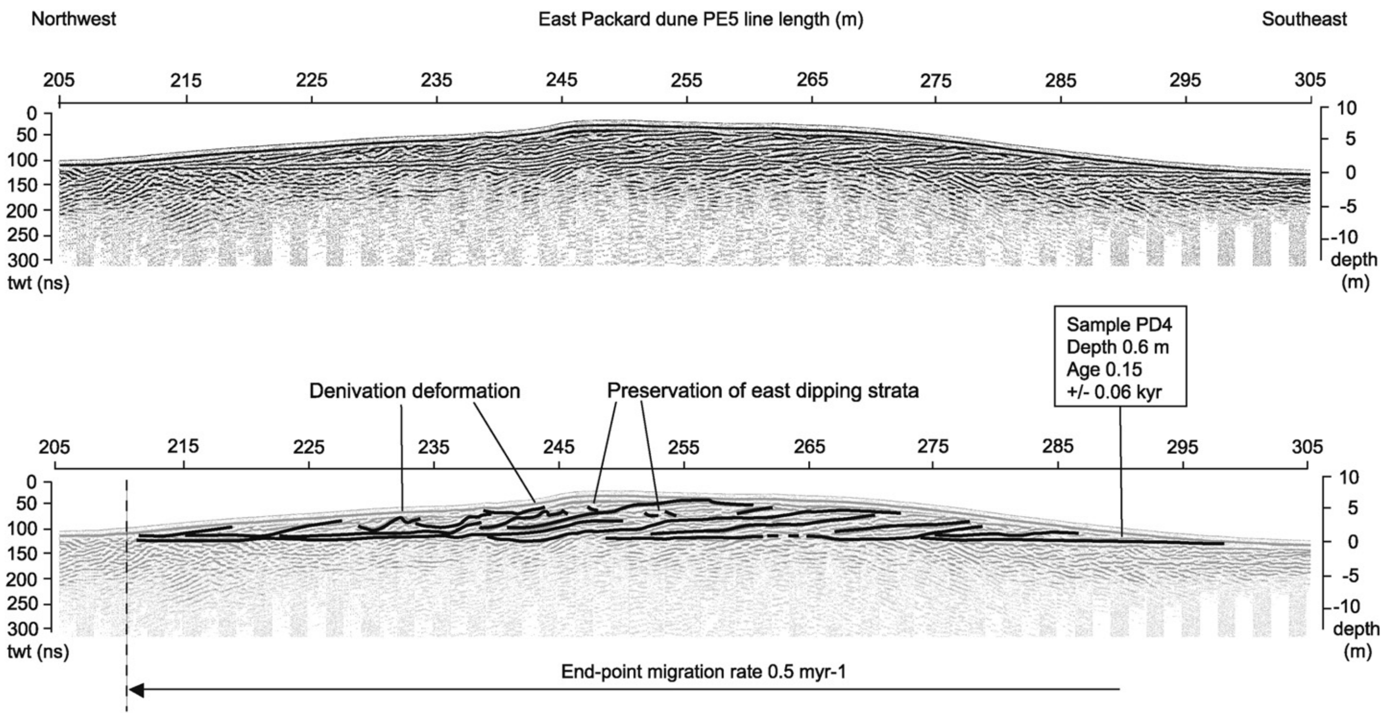

Fig. 6. PE5 has a broadly symmetrical cross-section with the slip-face close to the dune crest. The 200 MHz GPR profile shows inclined tangential reflections from cross-strata dipping towards the NW and irregular reflections from denivation deformation. There is limited evidence for preservation of east dipping strata formed by west winds. An OSL sample from 292 m has an age of 150 ± 62 yr which is used to calculate an end-point migration rate of 0.6 m/yr. Vertical exaggeration ×2.

migrates onto dune PE3. An OSL sample from a depth of 0.46 m at 150 m along the GPR profile has provided an age of 0.16 ± 0.02 kyr (Fig. 5). Projecting this age forwards to the base of the dune slip-face at 103 m indicates that the dune has migrated ca. 47 m in the past 160 yr to give an end-point migration rate of ca. 0.3 m/yr. This is much faster than the migration rate for PE3 and consistent with the observation that PE4 is superposed upon and migrating over PE3, and is consistent with observations that smaller dunes migrate faster than larger dunes (e.g. Cook et al., 1993; Jimenez et al., 1999).

6.3. Eastern Packard dune PE5

PE5 is a transverse dune oriented NE–SW adjacent to the till and glaciofluvial sediments of the Lower Victoria Valley. The dune has a convex profile with a NW facing slip-face close to the dune crest. Melting of snow layers in the lee of the crest created small-scale niveo-aeolian deformation features observed in the field. The 200 MHz GPR profile shows low-angle, inclined tangential, and irregular reflections with the reflection pattern indicating that the dune is a compound form with one transverse dune superimposed upon another (Fig. 6). Each dune contains inclined tangential reflections that dip towards the NW indicating migration from SE to NW. The contact between the two dunes is marked by a sub-horizontal bounding surface (Fig. 6). The irregular reflections are interpreted as deformed strata formed by the partial melting and deformation of interbedded snow and sand layers. An OSL sample from the trailing edge of the dune at a depth of 0.6 m at 290 m along the GPR profile gave an age of 0.15 ± 0.06 kyr. Projecting this age forward through the dune to an equivalent position on the toe of the dune at 212 m on the GPR profile gave an end-point migration rate of ca. 0.5 m/yr.

6.4. Western Packard dune PW1

PW1 is a transverse dune that is climbing onto a till ridge similar to the dune shown in Fig. 2. It has an asymmetric cross-section with a slip-face facing towards the west. The 200 MHz GPR profile shows low-angle inclined, sub-horizontal and inclined tangential bounding surfaces (Fig. 7). The vertical stacking pattern of sub-horizontal and low-angle inclined bounding surfaces in the middle and the lower parts of the dune indicate vertical dune aggradation. The aggradation is attributed to accretion of superposed dune sediments. It is possible that the vertical aggradation of the dune is a product of dune stabilisation by permafrost where ice cements have helped to stabilise the dune. Ice cements have quite literally frozen the dune sediments. The inclined tangential surfaces which are apparent in the upper parts of the dune and to the west of 55 m on the GPR profile (Fig. 7) indicate dune migration from east to west. OSL samples 1C, 1D, 1E and 1F, collected from pits excavated into the stoss-side of the dune, have been dated at 0.27 ± 0.12, 0.28 ± 0.05, 0.05 ± 0.01, and −0.09 ± 0.10 kyr, respectively. Sample 1F has a negative age estimate with a large error which overlaps zero age (−0.09 ± 0.10 kyr) and is effectively modern sand. Since this sample has a negative age estimate, it is not included in the subsequent analysis of dune migration rates. The remaining age estimates are used to calculate a rate of dune migration based upon sample age and the horizontal distance to the slip-face on the lee-side of the dune on the GPR profile (Fig. 7). The calculated end-point migration rates are 1.3 m/yr, 0.3 m/yr, and 0.4 m/yr, respectively. This is the only dune with multiple OSL ages and the migration rates here are equivalent to those calculated from individual dunes on the eastern side of Packard stream.

6.5. Western Packard dune PW2

PW2 is a transverse dune with an asymmetric cross-section, west facing slip-face and meltwater pools in the lee of the dune. The GPR profile shows low-angle sub-horizontal and inclined tangential reflections interpreted as bounding surfaces and sets of cross-stratification (Fig. 8). The inclined reflections dip towards the west indicating dune migration from east to west. One reflection close to the crest of the dune dips towards the east due to dune reversal during the previous winter. An OSL sample from a depth of 0.52 m at the eastern side of the dune at 86 m along the GPR profile has an age of 0.07 ±

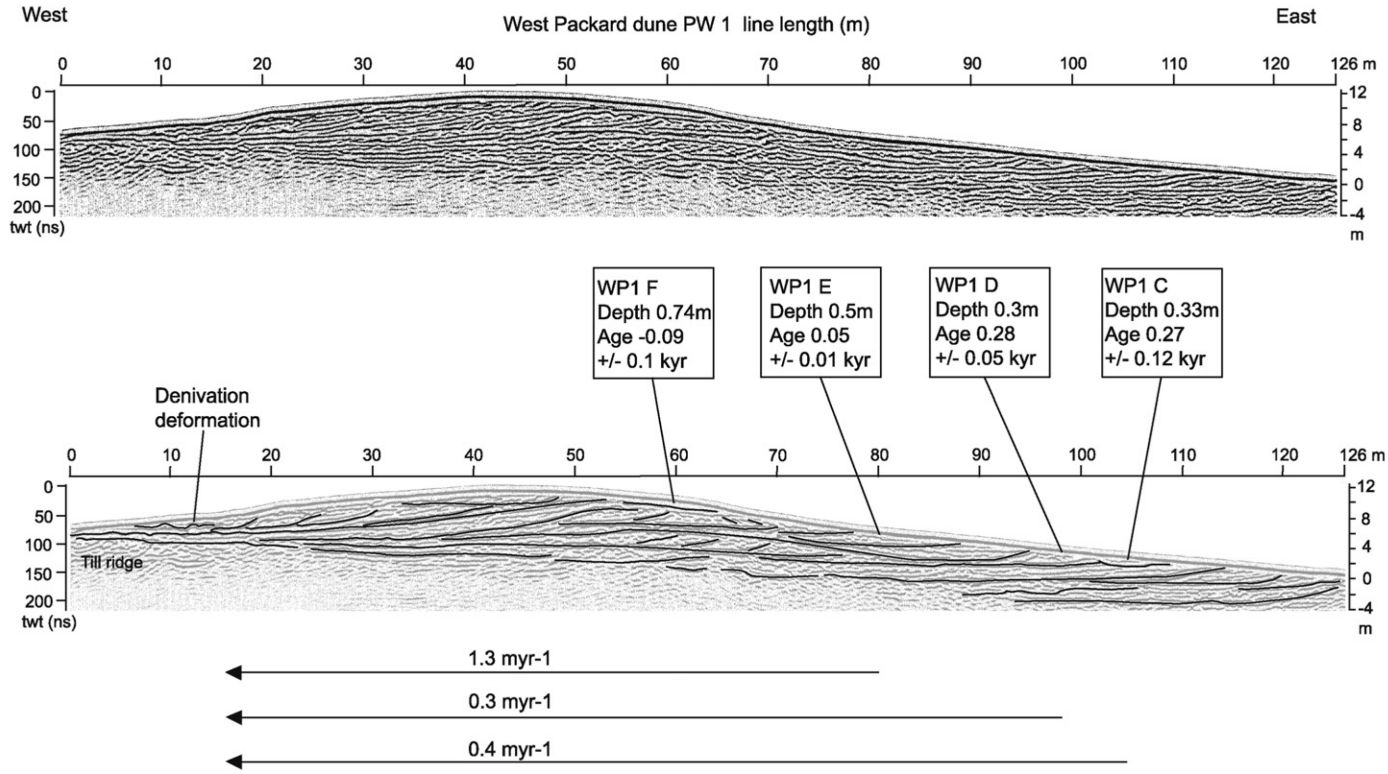

Fig. 7. A 200 MHz GPR profile, PW1, shows low-angle inclined and inclined tangential reflections from bounding surfaces and sets of cross-stratification. The stacking of sub-horizontal bounding surfaces indicates vertical aggradation, while inclined surfaces indicate dune migration from east to west. OSL ages from four locations on the dune are consistent with the stratigraphy of the dune younging from west to east, in the direction of dune migration. End-point migration rates calculated from the dune OSL age and distance to the slip-face on the west side of the dune vary between 0.3 and 1.3 m/yr. The youngest sample (WP1Fb) has a negative age with large errors and was excluded from the overall analysis of dune age and migration. Vertical exaggeration ×1.3.

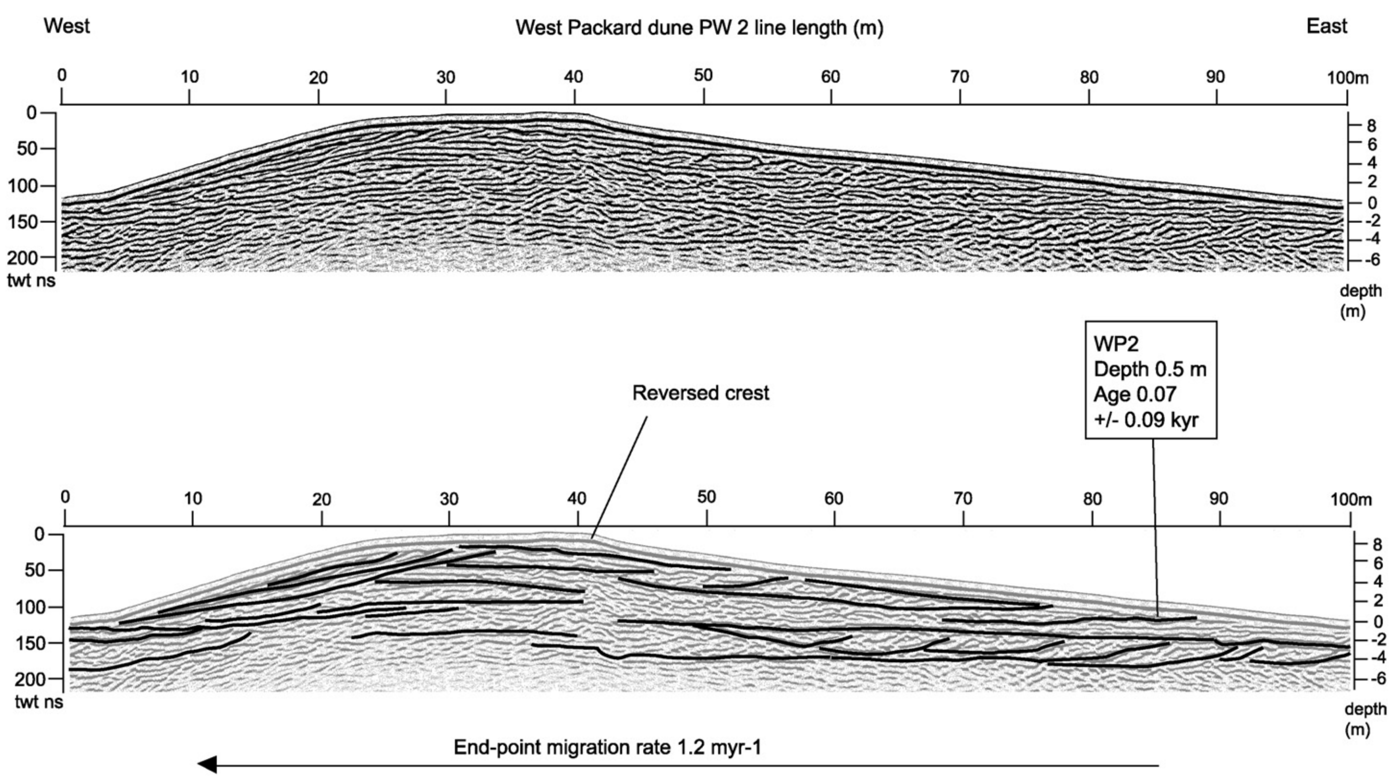

Fig. 8. PW2 is a transverse dune with an asymmetric cross-section with the crest displaced towards the west due to the effects of the previous winter's wind reversal. The 200 MHz GPR profile shows low-angle sub-horizontal and inclined reflections interpreted as bounding surfaces and sets of cross-stratification. The inclined reflections dip towards the west, indicating dune migration from east to west. One reflection close to the crest of the dune dips towards the east due to dune reversal during the previous winter. An OSL sample from 86 m gives an end-point migration rate of ca. 1.2 m/yr. Vertical exaggeration ×1.3.

0.03 kyr. Projecting this age through to the dune slip-face at 6 m along the GPR profile gives an end-point migration rate of 1.2 m/yr.

6.6. Western Packard dune PW3

PW3 is a transverse dune which is attached to a till ridge at its northern end. The west facing slope is relatively steep while the lower angle east facing stoss slope grades off into a flat interdune area into which the Packard stream occasionally flows. The GPR profile shows continuous sub-horizontal reflections within most of the dune, with inclined reflections on the west side (Fig. 9). The sub-horizontal reflections are interpreted as bounding surfaces where the dune has been reshaped by reversing winds and then aggraded vertically. This interpretation is supported by low-angle inclined reflections dipping towards the east that indicate deposition from westerly winds, which may also have deflated the dune crest creating the bounding surface. The inclined reflections on the western side of the dune dip towards the west and are interpreted as foresets deposited on the west facing lee-side slip-face when winds were blowing from the east. An OSL sample from a depth of 0.8 m at 34 m along the GPR profile gave an age of 0.09 ± 0.03 kyr. Projecting this age to the dune slip-face at 5 m along the GPR profile indicates that the dune has migrated 29 m within the past ca. 90 yr giving an end-point migration rate of ca. 0.3 m/yr.

7. Discussion

7.1. Dune ages

Both GPR imaging of the subsurface sediments and OSL dating of phases of dune aggradation have been shown to give good results in the frozen dunes from the Victoria Valley, Antarctica. Sample locations were selected for dating using OSL based upon the stratigraphic relationships interpreted from the GPR profiles. Although the OSL ages are young, and the OSL signal is very dim, with consequent large errors on the ages, where samples were taken from the same dune (e.g. PW1) the ages are in a consistent stratigraphic order which gives confidence to the subsequent interpretation of dune ages and rates of dune migration. In this study the depth of sampling was limited by environmental regulations which state that soil pits should be 0.5 m × 0.5 m and ice cemented sand layers through which we were unable to dig by hand. There is more, as yet undated, aeolian stratigraphy within the west Packard dunes, which might include older dune deposits.

7.2. GPR in frozen dunes on Earth and Mars

GPR has been proven previously to provide high resolution images of aeolian strata in desert dunes (e.g. Bristow et al., 2005, 2007). The results of this study demonstrate that GPR performs equally well, and sometimes better, in frozen sand, providing excellent images of dune strata. The results have positive implications for potential GPR surveys of aeolian strata on Mars. A GPR profile across the Lake Vida dune images dune stratigraphy to a depth of at least 70 m (Fig. 10), which is almost double the maximum depth of penetration for 100 MHz antennas determined in experiments by Smith and Jol (1995). The high quality of the profile and very high depth of penetration are attributed to the lack of liquid water in the Antarctic sand dunes. Sand dunes on Mars are unlikely to contain liquid water due to the cold and arid conditions on the planet's surface. The absence of liquid water should result in less signal attenuation and increased depths of signal penetration on Mars (Ori and Ogliani, 1996). The results shown here contrast with some other GPR surveys of Mars analogues on Earth where there has been high attenuation e.g. Heggy et al. (2006a,b). Our results suggest that sand dunes on Mars would be good targets for GPR surveys with low attenuation and well defined stratigraphy.

7.3. Bounding surfaces and wind reversals

GPR profiles collected across the Packard dunes image the sedimentary structures revealing a complex internal structure with many low-angle bounding surfaces within the dunes. The bounding surfaces are mostly attributed to reworking by seasonally reversing winds which reshape the dunes (Fig. 11). During the summer months easterly winds produce a west dipping slip-face. However, westerly winds can reshape the slip-face, rework sand from the dune crest and

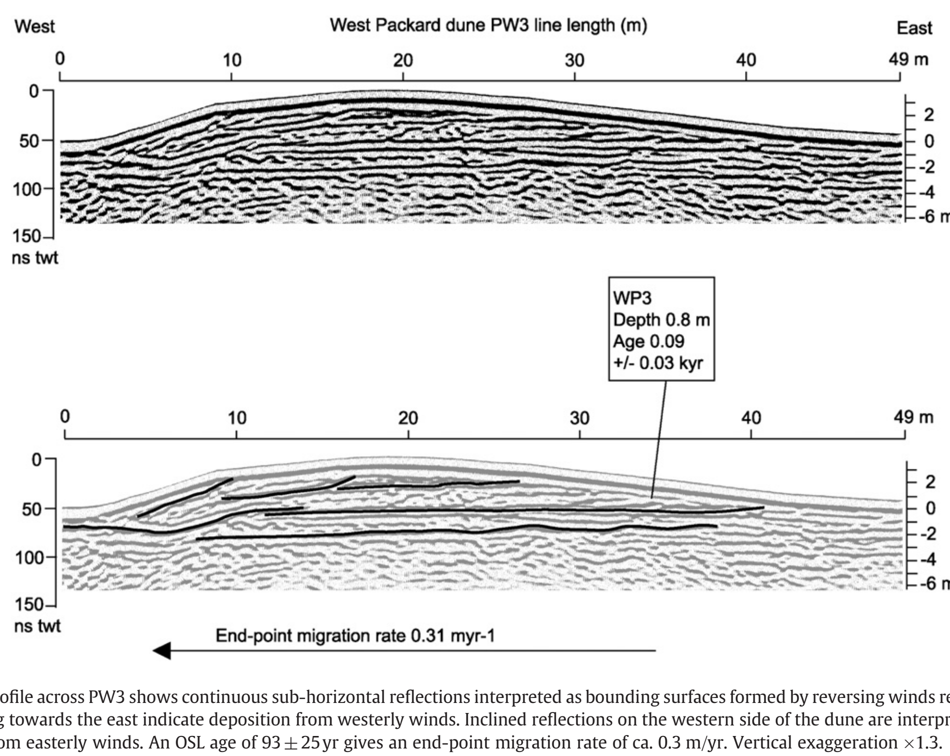

Fig. 9. The 200 MHz GPR profile across PW3 shows continuous sub-horizontal reflections interpreted as bounding surfaces formed by reversing winds reshaping the dune. Low-angle inclined reflections dipping towards the east indicate deposition from westerly winds. Inclined reflections on the western side of the dune are interpreted as foresets deposited on the lee-side of the dune from easterly winds. An OSL age of 93 ± 25 yr gives an end-point migration rate of ca. 0.3 m/yr. Vertical exaggeration ×1.3.

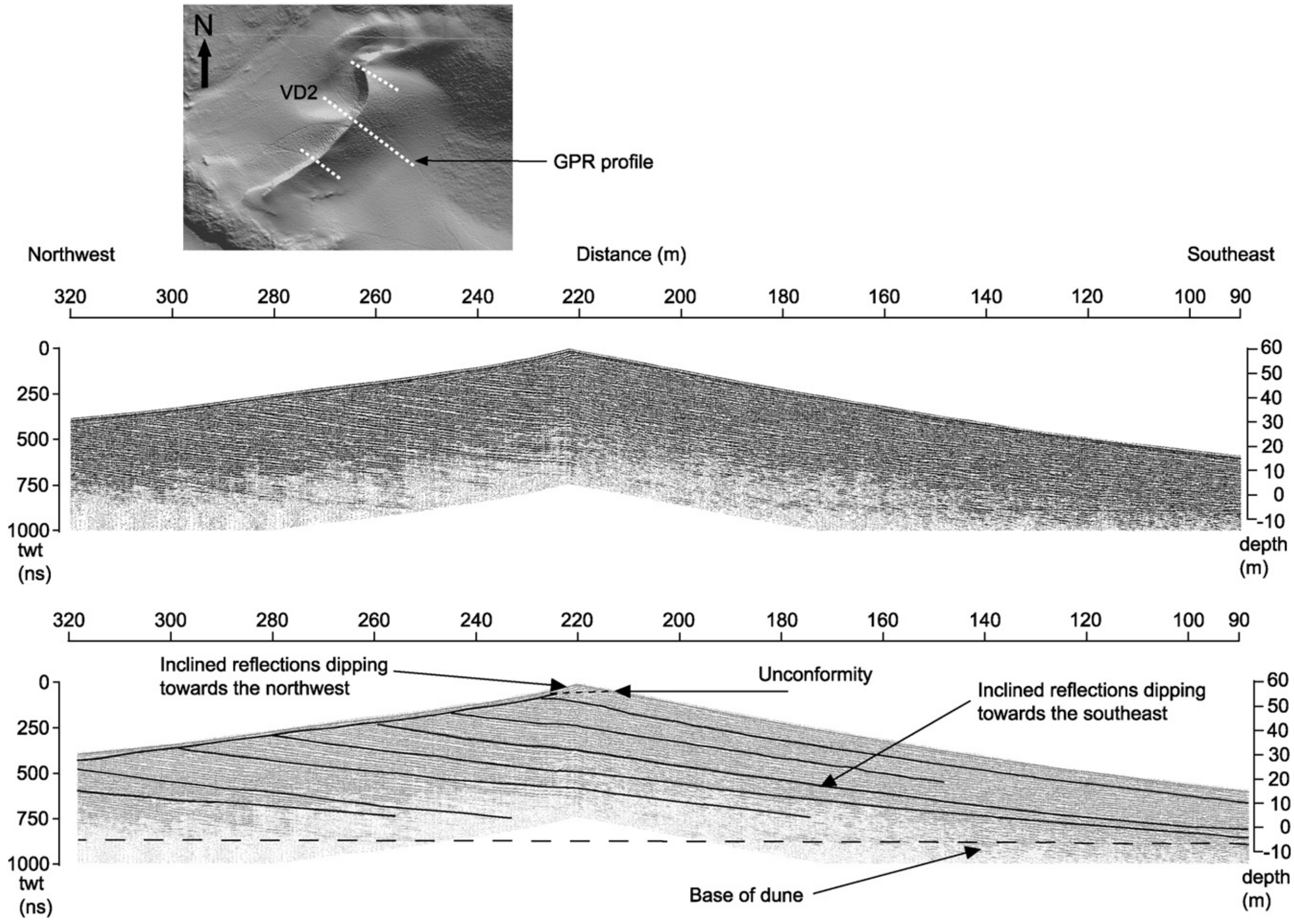

Fig. 10. Part of a 100 MHz GPR profile, VD2, across the Lake Vida dune reveals strata dipping from west to east, indicating that the dune has been accreting in that direction. Strata within the dune are imaged to a depth of over 70 m which is almost twice the maximum depth of penetration achieved in experiments by Smith and Jol (1995). The excellent depth of penetration and resolution of sedimentary strata are due to low attenuation and the lack of liquid water in the sand dunes in Antarctica.

deposit sand on what would be the stoss slope during the prevailing easterly summer winds (Fig. 11). The resumption of easterly winds switches the crest migration and re-establishes a west facing slip-face with cross-strata downlapping onto the bounding surface (Fig. 11). Inclined reflections usually dip towards the west indicating deposition on the lee-side of the dunes during easterly winds. Eastward dipping inclined reflections are less common, and where observed they are found close to the dune crest (e.g. PE1 and PE3; Figs. 5 and 7). Eastward dipping strata can be observed close to the crest of the dunes on the GPR profiles and have been described previously from trenches on dunes (Lindsay, 1973; Selby et al., 1974) and in the interdune areas (Miotke, 1985). However, there appears to be very little eastward dipping strata preserved at depth within the Packard dunes. The dominant dune-forming wind in the Packard dunes is therefore the easterly wind that blows inland from the Ross Ice Shelf during the summer months. Our results confirm the observations of Lindsay (1973) that the main period of dune growth occurs when the wind is from the east.

7.4. Bounding surfaces and superposed dunes

The very low-angle, sub-horizontal bounding surfaces within the dunes PW1, PW2 and PW3 indicate that the dunes have been eroded and then aggraded vertically as well as migrating downwind. The vertical aggradation may have been aided by the presence of compound transverse dunes with superposed dunes migrating over older dunes, as observed at PE3 and PE4. Analysis of historic aerial photographs by Bourke et al. (2009) identified variable rates of dune migration, which led to dune merging, lateral linking and absorption within the eastern part of the dune field. Migration of superposed dunes, dune merging and absorption could well have produced the sub-horizontal bounding surfaces seen in some dunes. Given its small size, it is most likely that the horizontal bounding surfaces in PW3 are also a function of wind reversals because it is too small to support superposed dunes.

7.5. Ice cements and dune morphology

The presence of ice cements within the frozen dunes probably prevents more extensive deflation during the winter months when the temperatures are extremely cold; winter temperatures reach −50 °C in the Victoria Valley, which has a mean annual temperature of −30 °C at Lake Vida (Doran et al., 2002). The ice cement helps to stabilise the dune forms and reduce dune mobility. It also appears to limit crest reversal and result in flattening of dune tops (e.g. PE1). Evidence from bounding surfaces and interbedded snow and sand strata demonstrates that the dunes are reworked during the winter months. It is likely that, when the dunes are not covered by snow, sublimation occurs in the hyper-arid conditions in Antarctica, and this makes sand available for aeolian transport during the winter months when temperatures almost never rise above freezing.

7.6. Solar radiation forces summer sand movement

There is a causal link between surface melting and the easterly winds which are the dominant winds with the Victoria Valley during

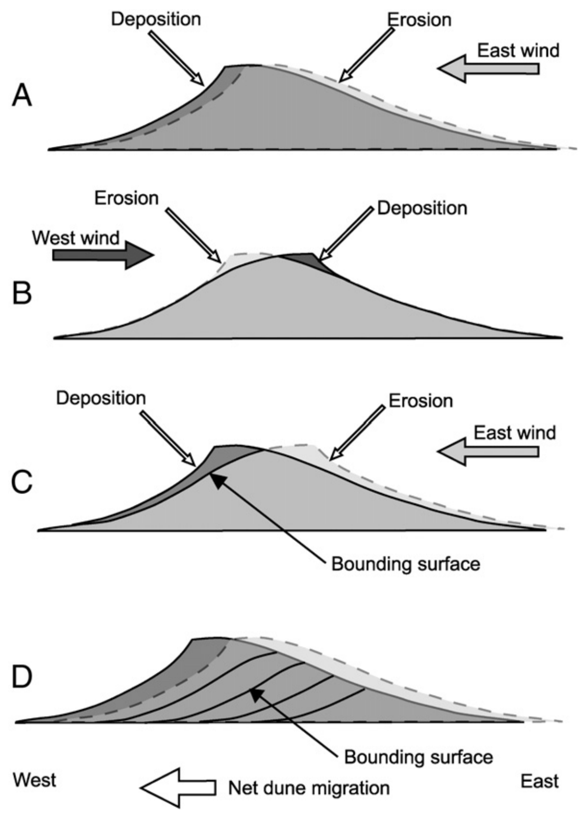

Fig. 11. Sketch illustrating the effects of reversing winds on dune morphology and dune migration. A) Deposition on the west facing slope during summer easterly winds. B) Dune is reshaped by west wind, with reworking of dune crest and deposition on the east facing slope during winter westerly winds. (C) Summer profile re-established under the dominant easterly dune-forming winds. Burial of the reshaped surface results in the formation of bounding surfaces as imaged on GPR profiles. D) Net dune migration is from east to west.

the summer months. This is because the easterly winds are "sea breezes" driven by solar radiation heating the valley floor (Nylen et al., 2004). The solar radiation which heats the valley floor promoting easterly winds also melts the frozen sand on the dunes, liberating sand and making it available for transport. Thus solar radiation has a multiplying effect on aeolian sand transport because solar radiation heats the surface of the valley floor generating wind and thereby increasing the potential for aeolian sediment transport, whilst at the same time melting the ice cement in frozen dune sand, increasing the supply of sediment available for wind deflation. Speirs et al. (2008) report warming from föehn winds, where increased temperature is accompanied by a reduction in relative humidity as well as an increase in wind velocity. This combination of physical factors also results in an increase in aeolian sand transport.

7.7. Migration of frozen dunes

Lindsay (1973) argued that because the dune cores were frozen there would be very little dune migration. However, Calkin and Rutford (1974) used photogrammetry and field observations to determine rates of dune migration. They measured the displacement of 205 dune crests and found an average movement of dune crest of 13 m between November 7th 1959 and January 27th 1962. This is effectively 13 m over four austral summers, giving an average migration rate of 3 m/yr. The mean of 72 measurements in the same area for the following seven year period was only 8 m (Calkin and Rutford, 1974), giving an average migration rate of 1.1 m/yr. Further field measurements over a 30 day period give an average of 11.2 cm/day (Miotke, 1985). More recent measurements over a four day period give a gross crest-line movement of 4.38 m (Speirs et al., 2008), equating to an average migration rate of 1.09 m/day. However, this rate does include a reversal in the direction of crest-line migration so that the net migration was only 0.12 m/day (Speirs et al., 2008).

Measurements of dune migration from historic aerial photographs and LiDAR data over a period of 40 yr from 1961 to 2001 average 1.5 m/yr (Bourke et al., 2009). End-point migration rates calculated form OSL ages in this study range from 0.05 to 1.3 m/yr, with an average of 0.5 m/yr. The average rate of migration calculated from OSL ages is less than that calculated from photogrammetry, and it is interesting to note an apparent decrease in the rate of migration with the length of time over which those measurements are made. Measurement of sand movement over a four year period (1959–1962) give an average of 3 m/yr, while measurements over a seven year period give an average of 1.1 m/yr. Although the 40 yr average is 1.5 m/yr (Bourke et al., 2009), the OSL ages used in this study are up to 1300 yr and give rates averaging ca. 0.5 m/yr. These results could suggest that dune migration rates have increased over time possibly in response to increasing temperatures in Antarctica (Bristow et al., in preparation). However, it is also possible that short-term rates are higher but more variable than longer term rates of dune migration, and the results presented here are probably realistic for the longer term (decadal to centennial) rates of dune migration in the Packard dunefield.

Rates of dune migration reported for warm desert dunes of similar height are 10 to 30 m/yr (Cook et al., 1993; Thomas, 1997). In comparison, the rates of dune migration reported for the Packard dunes are significantly lower and this is attributed to the combination of reversing winds and the cold climate, both of which act to reduce the net migration rate. The reversing winds cause crest reversal, reshape the dunes, and transport sand from the lee to the stoss slope. The summer winds have to undo the work of the winter wind reversals before dune progradation can be re-established, thereby reducing the net dune migration. The cold climate freezes the dunes, reducing the potential for sand entrainment and aeolian sediment transport. Thus, the rate of net dune migration is limited by the cold climate of the McMurdo Dry Valleys, Antarctica.

The westward migration of dunes in the Packard dune field contrasts with the neighbouring whaleback dunes which appear to be extending from west to east (Bristow et al., 2009), and the Lake Vida dune which contains east dipping strata (Fig. 10). The presence of dunefields in the same valley with opposing migration directions is attributed to a combination of topographic steering of the more powerful westerly winds along the axis of the valley where the whaleback dunes are located as well as drag against the valley wall. The Packard dunes which are located along the northern side of the valley, are thus partially sheltered from the west winds. Due to the curvature of the Lower Victoria Valley the Lake Vida dune is partially protected from the east winds but exposed to the west winds. The whaleback dunes which lie in the middle of the valley are exposed to both east and west winds but show net migration towards the east. Three dunefields within the same valley experience different wind regimes due to topographic steering of the winds and drag against the valley walls. The westerly winds are the dominant dune-forming winds on the whaleback dunes and Lake Vida dune, but the east winds are the dominant dune-forming winds on the Packard dunes.

8. Conclusions

Ground-penetrating radar (GPR) works well in frozen dune sand and successfully images the internal structures of reversing dunes. Depths of penetration exceed the maximum depths of penetration achieved in the experiments of Smith and Jol (1995). The results indicate that there is potential to image aeolian stratigraphy on Mars using GPR.

GPR profiles show low-angle bounding surfaces dipping in the direction of dune migration. These bounding surfaces record reshaping of the dunes during the winter months. The packages of sand between the bounding surfaces accumulate during the summer months when the dune surface thaws, allowing increased aeolian sediment transport. During the summer months easterly winds blow inland from the Ross Sea Ice Shelf. This combination of easterly winds during the summer months and increased sand availability for transport due to surface melting and sublimation produces a westward migration of the dunes. Thus, the dominant westward migration of the Packard dunes in the summer months is assisted by a multiplying effect driven by increased solar radiation that increases sand supply by melting frozen sediment and generates winds due to warming of the valley floor.

Westerly winds that reshape the dune slip-face produce bounding surfaces and rework sand from the west facing slip-face and dune crest to form a coeval slip-face on the east side of the dune. These sediments are largely lost through deflation during the summer months but can be preserved locally within the dune stratigraphy.

Repeated wind reversals can produce flat topped dunes with near-symmetrical profiles in very low temperature environments where freezing helps to stabilise the sand.

During the winter months the dunes are frozen and partially covered by snow. We suggest that the snow cover and ice cements reduce sand entrainment, although sand may be released through sublimation. Thus, although the westerly winds are stronger during the winter they appear to have less effect because the dunes are frozen and stabilised by ice cements and snow cover at that time of year. Additional field studies are required to investigate sand transport and dune migration in the winter months.

The three dunefields within the Lower Victoria Valley experience different wind regimes due to topographic steering of the east and west winds, as well as drag along the valley wall. The Packard dunes are partially sheltered from the powerful westerly winds that sweep down the Lower Victoria Valley because they are located along the northern side of the valley at the foot of the valley wall. In this location the wind velocity is believed to be reduced due to a combination of wall drag and topographic steering around a bend in the valley which directs the westerly winds towards the centre of the Lower Victoria Valley.

Optical dating of sand-sized grains of quartz has been used successfully to determine the age of dune sands in Antarctica. Further sampling is required to determine the age of the whaleback dunes, the much larger Lake Vida dune and deeper parts of the Packard dunes which are predicted to contain older aeolian deposits extending the record of dune deposition.

Rates of dune migration calculated from OSL ages are less than those derived from photogrammetric studies of dune migration, and an order of magnitude less than the migration rates reported from warm, low-latitude, desert dunes of similar height and horizontal dimensions.

Acknowledgements

Fieldwork was undertaken with logistical support from the Antarctica New Zealand, as well as grants from Birkbeck Faculty of Science to Bristow, an Auckland Research Committee Grant 3607921 to Augustinus, a grant from the Office of Research and Sponsored Programs, University of Wisconsin-Eau Claire and a University of Auckland post graduate bursary, the Natasha Divich Memorial Award, and Education New Zealand Post Graduate Study Abroad Award grants to Wallis. The manuscript has benefited from the detailed and constructive criticism of two anonymous reviewers.

References

Adamiec, G., Aitken, M.J., 1998. Dose-rate conversion factors: update. Ancient TL 16, 37–50.

Aitken, M.J., 1985. Thermoluminescence Dating. Academic Press.

Arcone, S.A., Prentice, M.L., Delaney, A.J., 2002. Stratigraphic profiling with ground-penetrating radar in permafrost: a review of possible analogs for Mars. J. Geophys. Res. 107 (E11), 5108. doi:10.1029/2002JE001906.

Ayling, B.F., McGowan, H.A., 2006. Niveo-eolian sediment deposits in coastal south Victoria land, Antarctica: indicators of regional variability in weather and climate. Arct. Antarct. Alp. Res. 38, 313–324.

Bateman, M.D., Murton, J.B., 2006. The chronostratigraphy of Late Pleistocene glacial and periglacial aeolian activity in the Tukoyaktuk Coastlands, NWT, Canada. Quat. Sci. Rev. 25, 2552–2568.

Bourke, M.C., Ewing, R.C., Finnegan, D., McGowan, H.A., 2009. Sand dune movement in the Victoria Valley, Antarctica. Geomorphology 109, 148–160.

Bristow, C.S., 2009. Ground penetrating radar in aeolian dune sands. In: Jol, H.M. (Ed.), Ground Penetrating Radar Theory and Applications. Elsevier Science Ltd.

Bristow, C.S., Augustinus, P., Rhodes, E., Wallis, I.C., Jol, H.M., in preparation. Climate change forces re-activation of a polar dunefield, Victoria Valley, Antarctica.

Bristow, C.S., Bailey, S.D., Lancaster, N., 2000a. The sedimentary structure of linear sand dunes. Nature 406, 56–59.

Bristow, C.S., Chroston, P.N., Bailey, S.D., 2000b. The structure and development of foredunes on a locally prograding coast: insights from ground penetrating radar surveys, Norfolk, England. Sedimentology 47, 923–944.

Bristow, C.S., Duller, G.A.T., Lancaster, N., 2007. Age and dynamics of linear dunes in the Namib Desert. Geology 35, 555–558. doi:10.1130/G23369A.

Bristow, C.S., Jol, H.M., Augustinus, P., Wallis, I.C., 2009. Slipfaceless 'whaleback' dunes in a polar desert, Victoria Valley, Antarctica: insights from ground penetrating radar. Geomorphology.

Bristow, C.S., Lancaster, N., Duller, G.A.T., 2005. Combining ground penetrating radar surveys and optical dating to determine dune migration in Namibia. J. Geol. Soc. 162, 315–322.

Bristow, C.S., Pugh, J., Goodall, T., 1996. Internal structure of aeolian dunes in Abu Dhabi determined using ground penetrating radar. Sedimentology 43, 995–1003.

Calkin, P.E., Rutford, R.H., 1974. The sand dunes of Victoria Valley, Antarctica. Geogr. Rev. 64, 189–216.

Ciarletti, V., Corbel, C., Cais, F., Plettemeier, D., Hamran, S.E., Øyan, M., WISDOM team, 2009. Performances of the WISDOM GPR designed for the shallow sounding of Mars. 40th Lunar and Planetary Science Conference. The Woodlands, Texas. 2367.pdf.

Cook, R.U., Warren, A., Goudie, A.S., 1993. Desert Geomorphology. UCL Press, London. 526.

Dijkmans, J.W.A., 1990. Niveo-aeolian sedimentation and resulting sedimentary structures; Søndre Strømfjord area, Western Greenland. Permafrost Periglac. Process. 1, 83–96.

Doran, P.T., McKay, C.P., Clow, G.D., Dana, G.L., Fountain, A.G., Nylen, T.H., Lyons, W.B., 2002. Valley floor climatology observations form the McMurdo dry valleys, Antarctica 1968–2000. J. Geophys. Res. 107 (D24), 4772. doi:10.1029/2001JD002045.

Fenton, L., Toigo, A.D., Richardson, M.I., 2005. Aeolian processes in Proctor Crater on Mars: mesoscale modelling of dune-forming winds. J. Geophys. Res. 110, E06005. doi:10.1029/2004JE002309.

Good, T.R., Bryant, I.D., 1985. Fluvio-aeolian sedimentation—an example from Banks Island, NWT, Canada. Geogr. Ann. Ser. A 67, 33–46.

Grotzinger, J.P., Arvison, R.E., Bell III, J.F., Calvin, W., Clark, B.C., Fike, D.A., Golombek, M., Greely, R., Haldemann, A., Herkenhoff, K.E., Jolliff, B.L., Knoll, A.H., Malin, M., McLennan, S.M., Parker, T., Soderblom, L., Sohl-Dickstein, J.N., Squyres, S.W., Tosca, N.J., Watters, W.A., 2005. Stratigraphy and sedimentology of a dry to wet eolian depositional system, Burns formation, Meridiani Planum, Mars. Earth Planet. Sci. Lett. 240, 11–72.

Hayward, R.K., Mullins, K.F., Fenton, L.K., Hare, T.M., Titus, T.N., Bourke, M.C., Colaprete, A., Christensen, P.R., 2007. Mars global digital dune database and initial science results. U.S. Geological Survey Open-File Report 2007-1158, p. 57.

Heggy, E., Clifford, S.M., Grimm, R.E., Dinwiddie, C.L., Stamatakos, J.A., Gonzalez, S., 2006a. Low-frequency radar sounding investigations of the North Amargosa Desert, Nevada: a potential analog of conductive surface environments on Mars. J. Geophys. Res. 111, E06S03. doi:10.1029/2005JE002523.

Heggy, E., Clifford, S.M., Grimm, R.E., Dinwiddie, C.L., Wyrick, D.Y., Hill, B.E., 2006b. Ground-penetrating radar sounding of mafic lava inflows: assessing attenuation and scattering losses in Mars-analog volcanic terrains. J. Geophys. Res. 111, E06S04. doi:10.1029/2005JE002589.

Jimenez, J.A., Maia, L.P., Serra, J., Morais, J., 1999. Aeolian dune migration along the Ceara coast, north-eastern Brazil. Sedimentology 46, 689–701.

Kocurek, G.A., 1996. Desert aeolian systems. In: Reading, H.G. (Ed.), Sedimentary Environments: Processes, Facies and Stratigraphy, pp. 125–153.

Koster, E.A., 1988. Ancient and modern cold-climate aeolian sand deposition: a review. J. Quat. Sci. 3, 69–83.

Koster, E.A., Dijkmans, J.W.A., 1988. Niveo-aeolian deposits and denivation forms, with special reference to the Great Kobuk Sand Dunes, northwestern Alaska. Earth Surf. Proc. Land. 13, 153–170.

Lindsay, J.F., 1973. Reversing barchan dunes in Lower Victoria Valley, Antarctica. Geol. Soc. Am. Bull. 84, 1799–1806.

Malin, M.C., Carr, M.H., Danielson, G.E., Davies, M.E., Hartmann, W.K., Ingersoll, A.P., James, P.B., Masursky, H., McEwan, A.S., Soderblom, L.A., Thomas, P., Veverka, J., Caplinger, M.A., Ravine, M.A., Soulanille, Warren J.L., 1998. Early views of the Martian surface form the Mars Orbital Camera of the Mars Global Surveyor. Science 279, 1681–1685.

Mann, D.H., Heiser, P.A., Finney, B.P., 2002. Holocene history of the Great Kobuk Sand Dunes, northwestern Alaska. Quat. Sci. Rev. 21, 709–731.

McGowan, H.A., Speirs, J.C., 2008. The polar foehn of the Victoria Valley, Antarctica. Extended Abstract, 13th Conference on Mountain Meteorology. Wistler, BC, p. 6.

McKee, E.D., 1979. A study of Global Sand Seas. USGS Prof. Pap. 1052, 1–17.

McKendry, I.G., Lewthwaite, E.W.D., 1992. Summertime along-valley wind variations in the Wright Valley Antarctica. Int. J. Climatol. 12, 587–596.

McKenna-Neuman, C., Gilbert, R., 1986. Aeolian processes and landforms in glacio fluvial environments of southeastern Baffin Island, N.W.T., Canada. In: Nickling, W.G. (Ed.), Aeolian Geomorphology. Allen and Unwin, Boston, pp. 213–235.

Mejdahl, V., 1979. Thermoluminescence dating: beta dose attenuation in quartz grains. Archaeometry 21, 61–73.
Miotke, V.F.-D., 1985. Die Dünen im Victoria Valley, Victoria-Land, Antarktis. Ein Betrag zur äolischen Formung im extreme kalten Klima. Polarforschung 55, 79–125.
Morris, E.C., Holt, H.E., Mutch, T.A., Lindsay, J.F., 1972a. Mars analog studies in Wright and Victoria Valleys, Antarctica. Antarct. J. US 7, 113–114.
Morris, E.C., Mutch, T.A., Holt, H.E., 1972b. Atlas of geologic features in the dry valleys of South Victoria Land, Antarctica: possible analogs for Martian surface features. US Geological Survey Interagency report: Astrogeology.
Mountney, N., Russell, A.J., 2004. Sedimentology of cold-climate aeolian sandsheet deposits in the Askja region of northeast Iceland. Sed. Geol. 166, 223–244.
Murray, A.S., Wintle, A.G., 2000. Luminescence dating of quartz using an improved single-aliquot regenerative-dose protocol. Radiat. Meas. 32, 57–73.
Murray, A.S., Wintle, A.G., 2003. The single aliquot regenerative dose protocol: potential for improvements in reliability. Radiat. Meas. 37, 377–381.
Nylen, T.H., Fountain, A.G., Doran, P.T., 2004. Climatology of katabatic winds in the McMurdo dry valleys, southern Victoria land, Antarctica. J. Geophys. Res. 109, D03114. doi:10.1029/2003JD003937.
Ori, G.G., Ogliani, F., 1996. Potentiality of the ground-penetrating radar for the analysis of the stratigraphy and Sedimentology of Mars. Planet. Space Sci. 44, 1303–1315.
Plettemeier, D., Ciarletti, V., Hamran, S., Corbel, C., Linke, S., Benedix, W., 2009. Design and performance of the WISDOM antenna system aboard the ExoMars Rover. Geophys. Res. Abstr. 11 EGU2009-11693.
Prescott, J.R., Hutton, J.T., 1994. Cosmic ray contributions to dose rates for luminescence and ESR dating: large depths and long term time variations. Radiat. Meas. 23, 497–500.
Reynolds, J.M., 1997. An Introduction to Applied and Environmental Geophysics. Wiley, New York.
Rhodes, E.J., 2000. Observations of thermal transfer OSL signals in glacigenic quartz. Radiat. Meas. 32, 595–602.
Rhodes, E.J., 2007. Quartz single grain OSL sensitivity distributions: implications for multiple grain single aliquot dating. Geochronometria 26, 19–29.
Rhodes, E.J., Pownall, L., 1994. Zeroing of the OSL signal in quartz from young glaciofluvial sediments. Radiat. Meas. 23, 329–333.
Selby, M., Rains, R., Palmer, R., 1974. Eolian deposits of the ice-free, Victoria Valley, southern Victoria Land, Antarctica. NZ J. Geol. Geophys. 17, 543–562.
Seppälä, M., 2004. Wind as a Geomorphic Agent in Cold Climates. Cambridge University Press, Cambridge.
Smith, D.G., Jol, H.M., 1995. Ground penetrating radar: antenna frequencies and maximum probable depths of penetration in Quaternary sediments. J. Appl. Geophys. 33, 93–100.
Speirs, J.C., McGowan, H.A., Neil, D.T., 2008. Meteorological controls on sand transport and dune morphology in a polar-desert: Victoria Valley, Antarctica. Earth Surf. Proc. Land. 33, 1875–1891. doi:10.1002/esp. 1739.
Speirs, J.C., McGowan, H.A., Steinhoff, D.F., Bromwich, D.H., 2009. The polar foehn: a re-examination of downslope winds in the McMurdo Dry Valleys, Antarctica. 9th International Conference on Southern Hemisphere Meteorology and Oceanography, Melbourne, Australia.
Squyres, S.W., Arvidson, R.E., Bell, J.F.I.I.I., Bruckner, J., Cabrol, N.A., Calvin, W., Carr, M.H., Chistensen, P.R., Clark, B.C., Crumpler, L., Des Marais, D.J., d'Uston, C., Economou, T., Farmer, J., Farrand, W., Folkner, W., Golombeck, M., Gorevan, S., Grant, J.A., Greely, R., Grotzinger, J., Haskin, L., Herkenhoff, K.E., Hviid, S., Johnson, J., Klingelhofer, G., Knoll, A.H., Landis, G., Lemmon, M., Li, R., Madsen, M.B., Malin, M.C., McLennan, S.M., McSween, H.Y., Ming, D.W., Moersch, J., Morris, R.V., Parker, T., Rice Jr., J.W., Richter, L., Rieder, R., Sims, M., Smith, M., Smith, P., Soderblom, L.A., Sullivan, R., Wanke, H., Wdowiak, T., Wolff, M., Yen, A., 2004a. The Opportunity Rover's Athena science investigation at Meridiani Planum, Mars. Science 306, 1698–1703.
Squyres, S.W., Grotzinger, J.P., Arvidson, R.E., Bell, J.F.I.I.I., Calvin, W., Chistensen, P.R., Clark, B.C., Crisp, J.A., Farrand, W., Herkenhoff, K.E., Johnson, J.R., Klingelhofer, G., Knoll, A.H., McLennan, S.M., McSween, H.Y., Morris, R.V., Rice Jr., J.W., Rieder, R., Soderblom, L.A., 2004b. In situ evidence for an ancient aqueous environment at Meridiani Planum, Mars. Science 306, 1709–1714.
Thomas, D.S.G., 1997. Sand seas and aeolian bedforms, In: Thomas, D.S.G. (Ed.), Arid Zone Geomorphology: Process, Form and Change in Drylands, 2nd Edition. , pp. 373–412.
Webb, P.N., McKelvey, B.C., 1959. Geological Investigations in the South Victoria Land, Antarctica: Part 1 — Geology of Victoria Dry Valley. NZ J. Geol. Geophys. 2, 120–136.
Wintle, A.G., Murray, A.S., 2006. A review of quartz optically stimulated luminescence characteristics and their relevance in single-aliquot regeneration dating protocols. Radiat. Meas. 41, 369–391.